An Experimental Study of the Deformation of Aggregates

Aliesha Scott, Matt McGuire, and Larry Glasgow
Dept. of Chemical Engineering, Kansas State University, Manhattan, KS 66506

DOI 10.1002/aic.10720
Published online October 28, 2005 in Wiley InterScience (www.interscience.wiley.com).

Keywords: flocculation, floc deformation, aggregate compression, kaolin-polymer aggregates

Introduction

Flocculation is a part of many solid-liquid separation processes, with prominent examples found in water treatment, mineral processing, and bioseparations. However, the aggregates produced by typical flocculation processes are difficult to characterize. The interplay between nonlinear, stochastic hydrodynamics and multiple-level aggregation leads to complex and highly irregular structures. The components of large aggregates range in size from the primary particles to large flocs. Furthermore, these pieces may be physically connected to the structure at one or many attachment points. Voids, or interstitial spaces, range in scale over three orders of magnitude, from something less than the primary particle size (<1 μm) up to the size of the largest component (>1 mm). Large, inhomogeneous aggregates can have immediately adjacent components that react very differently to applied stress. Such aggregates also contain very little of the solid phase (often about 1% by volume) and a great deal of the liquid. The practicality of the overall separation process may depend upon how much effort must be expended to deform the structure and expel the liquid phase. In the study reported here, a technique is described by which both the applied compressive force and volume of the deforming structure are measured simultaneously for individual aggregates. This work offers the prospect of a more rational approach to optimizing the physicochemical environment during flocculation for improved solid-liquid separations.

Experimental Procedures

Large aggregates were formed by the flocculation of colloidal kaolin with a high-molecular weight, anionic polyelectrolyte. Since kaolin has a negative surface charge in water, floc formation occurred by polymer bridging, i.e., loops and tails of the adsorbed macromolecules physically connect closely proximate surfaces. For our usual experimental conditions, the Debye length, $r_{D,}$ averaged 1.7 nm (17 Å). Individual aggregates were transferred to a water-filled acrylic plastic cylinder with an inside diameter of 17 mm. A neutrally-buoyant piston with an outside diameter of 15.6 mm was positioned so the bottom surface just contacted the top of the aggregate structure. A computer-controlled stepper motor was then used to push a Sensotec compression load cell down onto the top of the piston; rates of travel ranged from 15 to 60 μm/s, and experiments were carried out with both continuous and intermittent piston motion. Load cell output was recorded with a Keithley data acquisition system and piston motion was terminated when the output exceeded 0.5 N (50,000 dynes). The deforming aggregate's shape and size were recorded simultaneously using an Olympus digital camera (front view) and a Sony digital camcorder (bottom view). Additional experimental detail and a schematic of the apparatus can be found in Glasgow.[1]

Experimental Tests of Surrogate Structures

So little is known about floc deformation and the concurrent expulsion of interstitial water that a number of more easily characterized surrogate materials were tested to establish a basis for comparison. For example, cylindrical polyurethane foam cores were cut with a diameter of 12 mm and a height of 12 mm. The distribution of cell (or pore) size was measured using digitized microvideographic stills and image analysis. The cell size distribution was bimodal, with significant clusters of probability at 250 and about 2500 μm. In fact, 37% of the measured cells had diameters between 100 and 500 μm, and another 22% of the cells were larger than 1800 μm. The piston was pushed down upon the saturated polyurethane core at a constant rate of 30 μm/s. Typical output from the compression load cell is included in Figure 1; the three regions of the resulting curve conform to the characterizations: elastic modulus, buckling, and compaction, as described by Weaire and Hutzler.[2] Weaire and Hutzler observed that the large nonlinear effects seen in such experiments arise from both the structure and the material. The relaxation process (following cessation of

Correspondence concerning this article should be addressed to L.A. Glasgow at glasgow@ksu.edu.

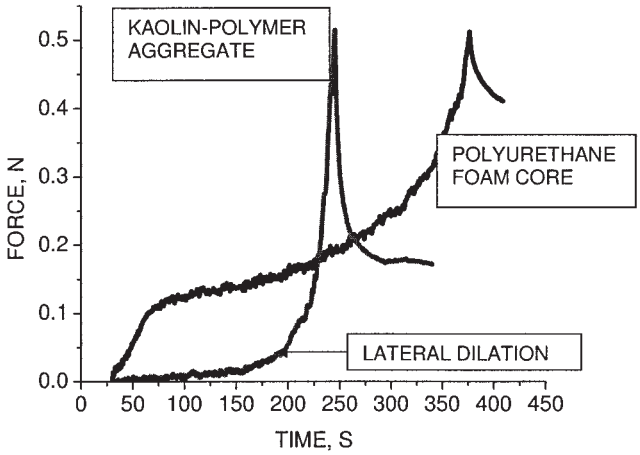

Figure 1. Comparison of measured force of compression for a large kaolin-polymer aggregate and the polyurethane foam core.

The piston speed was 30 μm/s in both cases. There are three distinct regimes of compression for the polyurethane foam.

piston motion) is also worthy of note; the measured force of compression decreased about 0.1 N (10,000 dynes) in 40 s. This is far less than the relaxation observed for kaolin-polymer aggregates.

Features of the Compressive Deformation of Kaolin-Polymer Aggregates

The results for surrogates like polyurethane foam provide a sharp contrast to the compressive deformation of large kaolin-polymer aggregates; this is underscored by Figure 1. For large flocs, the force of compression increases much more slowly at first (and nearly linearly), rising steeply as the aggregate structure begins to deform laterally; an example is included in Figure 1 (also with a piston velocity of 30 μm/s). Notice that the foam core offers much greater resistance in the early stages of the compression, while the kaolin-polymer aggregate is easily compressed initially. In the case of the latter, the compression process may be thought of as having four parts. First, some structural components get pushed into larger voids while the interparticle distance for most of the primary particles remains unchanged. Next, smaller components (and some primary particles) are forced closer together. with the accompanying expulsion of interstitial fluid. At this stage, however, the loops and tails of the adsorbed macromolecules are little affected. Third, many primary particles are forced closer together and conformations of the adsorbed macromolecules are changed. Finally, the permeability in the interstitial spaces is reduced so much that additional compression leads to lateral dilation of the structure.

Lyklema[3] noted that laterally interacting polymers tend to adsorb with one or two dangling tails. As the interparticle space is diminished, the permeability, k, is reduced by the projecting polymer loops and tails and tangential solvent flow is impeded. Cohen Stuart[4] pointed out that the porosity of the polymer layer increases (i.e., the segment density profile decreases monotonically) with distance from the clay surface. The effect of reduced permeability upon solvent flow can be accounted for with the Debye-Brinkman equation for the transient draining process:

$$\frac{\partial V_x}{\partial t} = -\frac{1}{\rho}\frac{\partial p}{\partial x} + v\left[\frac{\partial^2 V_x}{\partial y^2} - \frac{V_x}{k(y)}\right]. \quad (1)$$

Equation 1 was solved numerically for the moving boundary problem resulting from imposition of a constant pressure difference upon the passageway at t = 0. The permeability was taken to vary linearly from a minimum value at the wall to the maximum value at the centerline, y = δ/2. This means that passageway collapse leads to reduction of the centerline permeability, but the values assigned to the edges (y = 0 and y = δ) and the slope remain fixed. The top four curves shown in Figure 2 represent initial centerline permeabilities of 0.8, 2.0, 5.26, and 14.3 ($\times 10^{-12}$ m^2), respectively. For the bottom curve, k$\rightarrow\infty$.

As the structure is compressed, the loops and tails of the adsorbed macromolecules impede solvent flow and slow the response of the passageway to the imposed pressure difference. If the permeability is low enough, the draining process is so slow under applied force that the structure must accommodate additional stress with significant lateral dilation. We found it convenient to quantify this deformation with a dimensionless index:

$$DI = \frac{\sqrt{A_{proj}}}{h}, \quad (2)$$

where A_{proj} is the area determined from the bottom view and h is the aggregate height. DI can be plotted as a function of the cumulative work performed in the deformation of the polyurethane samples and the kaolin-polymer aggregates. Typically, 1×10^{-3} N·m were required to raise DI from 1 to 3 for the foam cores; DI $\approx$ 3 corresponds to a loss of volume of 60% in

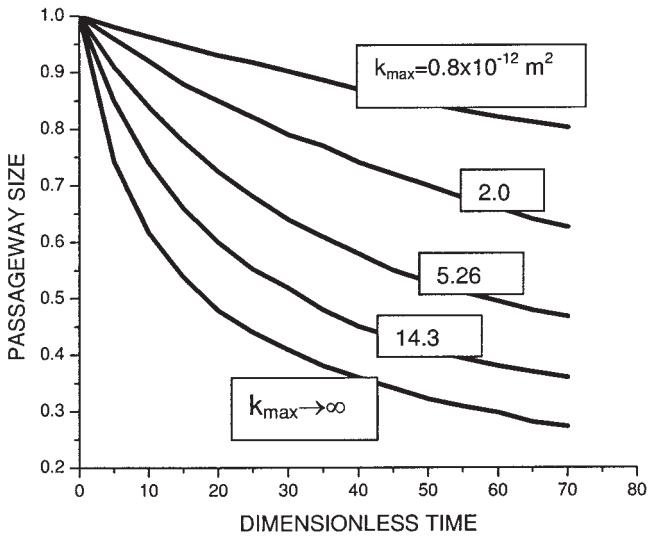

Figure 2. Results of the numerical computation δ/δ_0 as a function of dimensionless time, P_0t/μ.

The curves correspond to initial centerline permeabilities of 0.8, 2.0, 5.26, and 14.3 ($\times 10^{-12}$) m^2; the bottom curve is for $k_{max} \rightarrow \infty$.

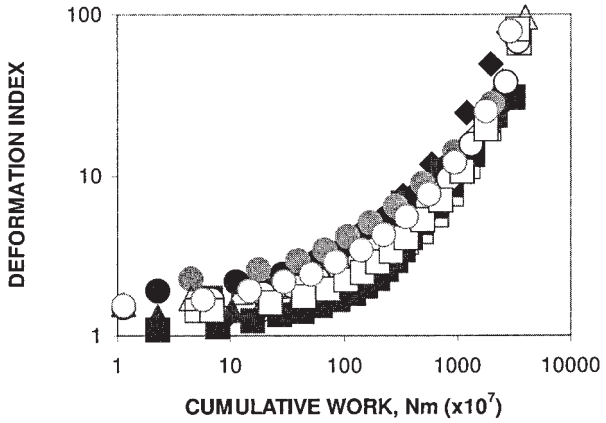

Figure 3. Deformation index as a function of cumulative work performed upon 12 large kaolin-polymer aggregates.

The piston speed for all trials was 30 μm/s.

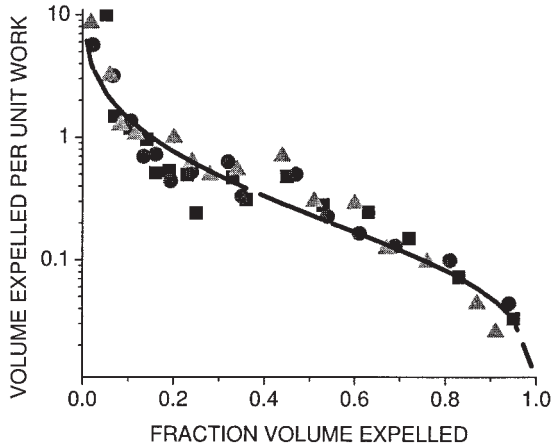

Figure 4. Volume of interstitial fluid expelled per unit work, V_w (m^3 per N·m × 100), as a function of the fractional volume expelled, F_v.

these cases. In contrast, the cumulative work required to raise DI to about 10 was only 1×10^{-4} N·m for large kaolin-polymer aggregates. A deformation index of 10 in this case corresponds approximately to a 65 to 75% loss of volume; data from 12 separate (kaolin-polymer) trials are shown in Figure 3. For large kaolin-polymer aggregates, a cumulative work of compression of about 4×10^{-4} N·m will produce a deformation index approaching 100. With the polyurethane foam surrogates, about 2×10^{-3} N·m will yield a DI of a little less than 10. The variability evident in Figure 3 is typical of these aggregate structures; it is a consequence of both the wide range of component sizes and the variation in number of contact points between the component and the central structure.

The diminishing expression of interstitial fluid is shown clearly by Figure 4, which contains experimental data from the compression of three large kaolin-polymer aggregates. By the time fractional volume expulsion ($F_v = 1 - V/V_0$) reaches about 95%, the rate of volume expelled per unit work (V_w) will have decreased by nearly three orders of magnitude. The data shown in Figure 4 are reasonably well-described by the empirical equation:

$$V_w \cong 0.1999(1 - F_v)^{0.37}\exp(-5.4F_v^{0.297}). \tag{3}$$

The leading constant (0.1999) has dimensions of m^3 per N·m. The constants and exponents in Eq. 3 were determined using sequential simplex to minimize the sum of the squares of the deviations. The data indicate an initial volume loss (expulsion) rate of about 0.1 m^3 per N·m of compression work for large kaolin-polymer aggregates. However, by the time one-half of the volume has been expelled, the loss rate is only about 0.0025 m^3 per N·m of work. Eq. 3 can be integrated to determine the average rate for volume expulsion per unit work; for limits on F_v of 0 and 25%, this average is 0.0159 m^3 per N·m. For limits of 0 and 98%, the average is only 0.0053 m^3 per N·m. In fact, when $(1 - V/V_0)$ reaches 95%, V_w is only about 0.0002 m^3 per N·m. These data are in accord with a well-known feature of liquid expulsion from water treatment plant residuals: Only about half of the water initially contained in the sludge can be removed easily by mechanical means.

We can better understand this problem by looking at the change in mean interparticle distance as the deforming aggregate loses volume through expulsion of interstitial fluid. The apparent density of a large kaolin-polymer aggregate is determined from the mass of clay and water comprising the structure:

$$\rho_{floc} = \frac{V_{clay}\rho_{clay} + V_w\rho_w}{V_{floc}}. \tag{4}$$

For the colloidal kaolin used in this study, $\bar{d}_p \approx 1.5$ μm and $\rho_{clay} \approx 2540$ kg/m^3. Since $V_w = V_{floc} - V_p n_p$, estimates for the aggregate density and size will allow determination of the number of primary kaolin particles (n_p) in the structure. We used settling velocity for a sample of large kaolin-polymer aggregates (with mean diameters between 2.3 and 5.9 mm) to estimate ρ_{floc}, neglecting the effect of permeability upon drag. Matsumoto and Suganuma[5] showed that if the ratio, $R_{floc}/k^{1/2}$ is greater than about 20, then permeability can be disregarded. Glasgow and Hsu[6] measured the permeability of large kaolin-polymer flocs and found values of k ranging from 10^{-12} to 10^{-11} m^2; accordingly, the minimum value for $R_{floc}/k^{1/2}$ in our study was over 300. The terminal velocity data yielded $\bar{\rho}_{floc} = 1058$ kg/m^3 with $\sigma = 7.49$ kg/m^3. If we select $\rho_{floc} = 1058$ kg/m^3 and $d_{floc} = 6$ mm, then $n_p = 2.41 \times 10^9$. The volume of

Table 1. Estimated Mean Interparticle Distance, *S*, for a Large (6 mm) Kaolin-Polymer Aggregate Undergoing Compressive Deformation

Volume Expelled, %	S, μm	$S_0 - S$, μm	F, N, Experim.
0	2.98	0	0
10	2.82	0.16	0.00328
20	2.66	0.32	0.00713
30	2.48	0.50	0.01373
40	2.28	0.70	0.02162
50	2.05	0.93	0.03050
60	1.80	1.18	0.04563
70	1.50	1.48	0.09150
80	1.12	1.86	0.19000
90	0.58	2.40	0.39066
95	0.15	2.83	0.51166

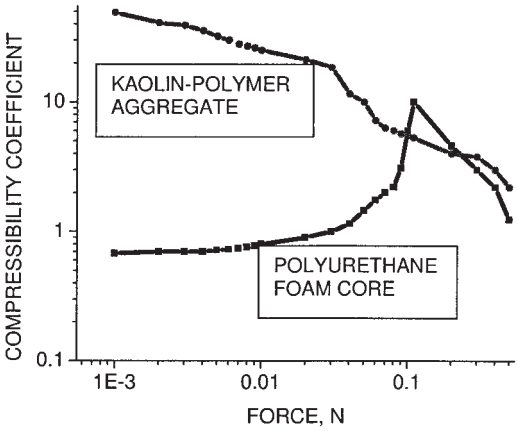

Figure 5. Composite compressibility coefficients (N^{-1}) for three kaolin-polymer aggregates and three trials with the polyurethane foam core as functions of the compressive force (dynes).

All data were obtained at a piston speed of 30 μm/s.

interstitial fluid associated with each primary particle can be estimated by dividing: V_w/n_p. If the kaolin plates are assumed to have spherical shape, then the average interparticle distance (S) for this example can be calculated: 2.98 μm. As the aggregate is compressed, interstitial fluid is expelled, volume is lost, and the average interparticle distance decreases. Computed results for this example are given in Table 1. The data in Table 1 show that a 20% loss in volume corresponds to 10.7% reduction in S; when 80% of the initial aggregate volume is expelled, S will be reduced by more than 60%. And for a 95% volume expulsion, the *mean* interparticle distance is reduced to 0.15 μm (150 nm).

We also found it useful to define a compressibility coefficient, β:

$$\beta = -\frac{1}{V}\frac{\partial V}{\partial F}, \tag{5}$$

where V is aggregate volume and F is applied compressive force; β has dimensions of reciprocal force (N^{-1}). For purely elastic behavior, β would be constant, but for large aggregates formed from colloidal kaolin we can expect β to decrease with increasing compression. On the other hand, for the surrogate polyurethane foam cores, the buckling regime will lead to a significant increase in β until cell compaction begins to dominate. These differences are readily apparent in Figure 5 in which composite data for three large kaolin-polymer aggregates and three separate trials with the polyurethane foam core are presented. These results show that β is initially nearly two orders of magnitude larger for the aggregates than for the foam core. However, by the end of the compression process, the compressibility coefficients are comparable.

Conclusions

The deformation of large kaolin-polymer aggregates has been studied in a piston-cylinder apparatus, measuring shape, volume, and force of compression simultaneously. A range of piston speeds and intermittent compression regimens were studied with the idea that the total work required for interstitial fluid expulsion could be minimized; however, the results did not produce a clear optimum.

In the initial stages of compression of flocs, there is little resistance to piston travel, and rate of volume expulsion per unit work is large. Once the larger voids have been filled by displaced subsidiary components, the volume expelled per unit work decreases slowly, and this persists until about 50 or 60% of the original aggregate volume has been lost. As the fraction of volume expelled exceeds about 60%, there is a good deal of lateral dilation and the work requirement for a fixed rate of volumetric expulsion increases steeply. This is attributed in part to the sharp reduction in permeability in the interstitial spaces as the loops and tails of the adsorbed macromolecules are crowded together.

Acknowledgments

This material is based upon work supported by the National Science Foundation under Grant No. CTS-0135468. The authors are grateful for this support. We would also like to recognize the assistance of Andrew R. Glasgow with computerized control of the stepper motor.

Literature Cited

1. Glasgow LA. Deformation of individual aggregates and flocs. *J Dispersion Sci and Technology.* 2003;24:715-720.
2. Weaire D, Hutzler S. *The Physics of Foams*. Oxford: Oxford University Press; 1999.
3. Lyklema J. Adsorption of polyelectrolytes and their effect on the interaction of colloid particles. In: *Modern Trends of Colloid Science in Chemistry and Biology*, Eicke HF, Ed.; 1985.
4. Cohen Stuart MA. Adsorbed polymers in colloidal systems: from statics to dynamics. *Polymer Journal.* 1991;23:669-682.
5. Matsumoto K, Suganuma A. Settling velocity of a permeable model floc. *Chemical Eng Sci.* 1977;32:445-447.
6. Glasgow LA, Hsu JP. Floc characteristics in water and wastewater treatment. *Particulate Sci and Technology.* 1984;2:285-303.

Manuscript received June 15, 2005, and revision received Sept. 27, 2005.